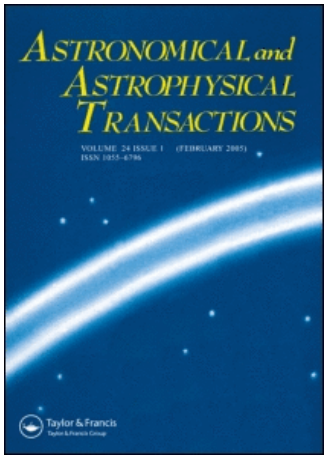

Astronomical & Astrophysical Transactions
The Journal of the Eurasian Astronomical Society
Publication details, including instructions for authors and subscription information:
http://www.informaworld.com/smpp/title~content=t713453505

WEAKLY MASS-LOADED ACCRETION DISCS

Yuri Shchekinov [a]
[a] Department of Physics, University of Rostov, Rostov on Don 344090, Russia.

Online Publication Date: 01 February 2003
To cite this Article: Shchekinov, Yuri (2003) 'WEAKLY MASS-LOADED ACCRETION DISCS', Astronomical & Astrophysical Transactions, 22:1, 81 - 93
To link to this article: DOI: 10.1080/1055679031000079610
URL: http://dx.doi.org/10.1080/1055679031000079610

Astronomical and Astrophysical Transactions,
2003, Vol. 22(1), pp. 81–93

Taylor & Francis
Taylor & Francis Group

WEAKLY MASS-LOADED ACCRETION DISCS

YURI A. SHCHEKINOV*

Department of Physics, University of Rostov, Rostov on Don 344090, Russia

(Received February 27, 2002)

Accretion discs with an additional mass input on the disc surface from the environment are considered in the limit of a low mass input rate, when the accretion flow remains Keplerian. Owing to dissipation of kinetic energy of the infalling gas, the disc temperature increases and can deviate significantly from standard temperature of reprocessing accretion discs in their outer regions. This increase in temperature produces an excess of emission in a long-wavelength range of the disc spectrum. An illustrative example of the spectrum of a weakly mass-loaded disc (the surface mass input rate $\dot{M}_{\rm load} \approx 1.5 \times 10^{-8} M_\odot\,{\rm year}^{-1}$) reasonably reproducing the far-infrared excess observed in CS Chameleon is given.

Keywords: Accretion discs; Additional mass input; Keplerian accretion flow; Far-infrared excess

1 INTRODUCTION

The dynamics of the multiphase interstellar medium are dominated by mass and momentum exchange between different phases. Ejection of mass into a diffuse component from a condensed phase changes the velocity of the bulk flow, increases pressure in the diffuse phase and heats the diffuse gas resulting from the conversion of kinetic energy of evaporated and destroyed clouds into thermal energy of the bulk medium (Cowie *et al.*, 1981; Hartquist *et al.*, 1986). As a result, loaded flows (i.e. the flows dominated by mass input from a condensed phase) can differ qualitatively from those in a homogeneous (monophase) medium. In the simplest approach, mass-loaded flows are described by dynamic equations with source terms. For accretion discs, mass loading corresponds physically to a continuing mass infall on the disc surface from the residual gas envelope.

The extremely inhomogeneous structure of the diffuse interstellar gas and molecular clouds shows self-similarity on the scales from 0.02 pc (the resolution threshold) to 100 pc (Falgarone *et al.*, 1991). It seems obvious that such self-similarity can extend to much smaller scales corresponding to protoplanetary condensations in accretion discs. (Note that the resolution limit, 0.02 pc, corresponds to planetary masses of clumps, approximately $10^{-4} M_\odot$.) One can expect that, in such conditions, clumpy gas from the debris of the parent molecular cloud will provide a continuing matter infall on the accretion protoplanetary disc already being formed. In a theoretical treatment of protoplanetary discs this circumstance is

*E-mail: yus@phys.rnd.runnet.ru

ISSN 1055-6796 print; ISSN 1476-3540 online
DOI: 10.1080/1055679031000079610

described by the source terms in mass and momentum equations (see for example Safronov and Vityazev (1983) and Papaloizou and Lin (1995)). Multiple C I and CO velocity components (Roberge *et al.*, 2000), Ca II absorptions (Barnes *et al.*, 2000) and emission in Fe II, S I, Si II, Ni II and C I lines (Lecavelier des Etangs *et al.*, 2000), observed in β Pictoris, are seemingly connected with the infall of clumpy gas on the disc. Similar detections of the infalling circumstellar gas have been reported for Herbig Ae/Be stars (Grinin *et al.*, 1996). One can assume that this phenomenon represents late stages of matter infall from a highly inhomogeneous primordial circumdisc cloud on to the accretion disc. If this is the case, with protoplanetary discs loaded by dense clumps infalling and passing through them, both the vertical and the radial structure of such discs, the accretion rate and the temperature distribution can differ considerably from those in homogeneous (monophase) discs. In this paper we analyse the properties of steady discs, concentrating mainly on the radial temperature distribution in a simple model of weak mass loading, when mass loading does not violate the Keplerian flow of the bulk motion. In Section 2.1 we describe the model; in Section 2.2 we formulate the basic equations describing the radial structure of thin accretion discs for the weak-mass-loading limit; in Section 2.3 we describe the solution of the energy equation, find the radial temperature distribution and discuss possible observational manifestations; the effects of the angular momentum input associated with mass loading on the temperature distribution are discussed in Section 2.4; Section 3 summarizes the results.

2 MODEL AND GOVERNING EQUATIONS

2.1 Model of Weakly Loaded Discs

As a model of a mass-loaded disc which admits simple analytical description, we shall accept the following: an accretion disc is surrounded by a spherical 'subsystem' of dense condensations formed of the debris of a parent cloud and orbiting around the central star (Figure 1). This subsystem can be in a quasistationary state either because the condensations are nearly dissipationless, or because an infinite (in practice, very massive) reservoir of gas replenishes dissipation of mass and energy. In the first case, the characteristic lifetime of the quasistationary orbits determined by interaction of the condensations with the diffuse component, with other condensations and with the disc itself must be much longer than the characteristic rotation period of the disc. For this to be fulfilled the following relations must hold:

$$N_{\rm i} \ll N_{\rm c}, \quad \langle N_{\rm c} \rangle \ll N_{\rm c}, \quad N_{\rm d} \ll N_{\rm c}, \tag{1}$$

where $N_{\rm i}$, $N_{\rm c}$ and $N_{\rm d}$ are the column densities of the diffuse intercloud gas over the whole circumdisc cloud, of a single clump and of the disc respectively; $\langle N_{\rm c} \rangle = f N_{\rm c}$, $f = \mathcal{N}_{\rm c} R_{\rm c}^2 / R^2$ is the covering factor of clumps, $R_{\rm c}$ is the clump radius, and R is the radius of the circumdisc cloud. These inequalities are definitely fulfilled for planetesimals or comet-like bodies. For gaseous clumps it is not so obvious, and one has to assume a sufficiently large density contrast in order that the clumps were long living and orbiting in a quasistationary manner. In the latter case when the clumps are not sufficiently dense, so that for instance $N_{\rm c} \approx N_{\rm d}$, and they are absorbed by the disc in a single encounter, the overall picture can be kept quasistationary owing to replenishment of the clumps from the surrounding molecular cloud as shown schematically in Figure 1. A gas reservoir with radius $R \approx 3$–$10\,{\rm pc}$ can support continuous mass infall during the time $t \approx 1$–$3\,{\rm M}$ years with the rate 10^{-7}–$10^{-6} M_\odot\,{\rm year}^{-1}$ if the mean density is only $n_{\rm c} f_{\rm v} \approx 0.03$–$0.3\,{\rm cm}^{-3}$, where $n_{\rm c}$ is

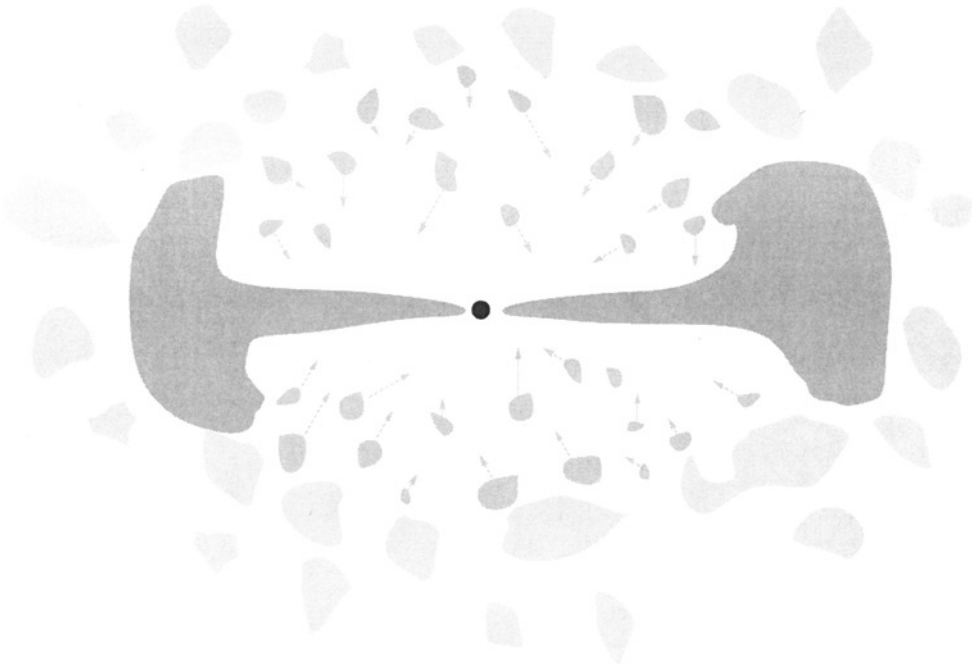

FIGURE 1 Schematic representation of the model: debris of the seed cloud falling down on the accretion protoplanetary disc.

the gas density in clumps and f_v is the volume filling factor of the clumps; the optical depth corresponding to the whole ensemble of such clumps is small; $\tau_c \approx 10^{-21} n_c f_v R \approx 0.03$. As we shall see below, mass loading, even with a mass rate one order of magnitude lower, can produce observable effects. We shall assume that the quasistationarity takes place in either way. With these assumptions the subsystem of clumps can be treated as stationary. When the clumps intersect the disc, they lose a fraction of their mass because of stripping under the action of the Rayleigh–Taylor instability (see the detailed discussion given by Hartquist *et al.* (1986) and Klein *et al.* (1994)). The subsystem of clumps is assumed to be at rest as a whole, that is $\langle \boldsymbol{v}_c(\boldsymbol{r}) \rangle = 0$, where the averaging is over the ensemble of clumps at given $\boldsymbol{r}$, such that the angular momentum input into the disc from destroying clumps is zero. The more general case with $\boldsymbol{v}_c = \boldsymbol{v}_c(\boldsymbol{r})$ will be discussed in Section 2.4.

2.2 Equations of Motions

In this framework the continuity equation for a thin disc is described by the equation

$$\frac{1}{R}\frac{\mathrm{d}}{\mathrm{d}R}(R\Sigma u_R) = \Psi, \tag{2}$$

where $\Sigma = \int_{-\infty}^{+\infty} \rho \, \mathrm{d}z$, $u_R = \int_{-\infty}^{+\infty} v_r \, \mathrm{d}z$ (the interrelation $\Sigma u_R = \int_{-\infty}^{+\infty} \rho v_r \, \mathrm{d}z$ is assumed as well), $\Psi = \int_{-\infty}^{+\infty} q \, \mathrm{d}z$, q ($\mathrm{g\,cm^{-3}\,s^{-1}}$) is the mass ejection rate from destroying clumps per unit volume. (In general, Ψ may represent not only mass loading due to destroying cloudlets, but also mass infall on to the disc from the envelope (Safronov and Vityazev, 1983), the

effects of the mass transfer stream in cataclysmic variable stars, and the mass loss through a wind (Papaloizou and Lin, 1995).)

The Navier–Stokes equation for the azimuthal component of a stationary disc with zero angular momentum input is written in the standard form (Shakura and Sunyaev, 1973; Pringle, 1981)

$$\frac{\mathrm{d}}{\mathrm{d}R}(\Sigma R^3 \Omega u_R) = \frac{\mathrm{d}}{\mathrm{d}R}\left(\nu \Sigma R^3 \frac{\mathrm{d}}{\mathrm{d}R}\Omega\right); \tag{3}$$

here $u_\phi = \Omega R$ is explicitly taken into account; $\Omega = \Omega(R)$ is the local angular velocity and ν is the kinematic viscosity. The change in the angular velocity Ω in one rotational period $T_\mathrm{R} = 2\pi/\Omega$ due to mass input is $|\Delta\Omega| \sim \Psi/\Sigma$. From the requirement that $|\Delta\Omega|/\Omega \ll 1$, one obtains the restriction on the mass loading, $\Psi \ll \Sigma\Omega/2\pi$, so that the ratio of the mass input rate $\dot{M}_\mathrm{p}$ associated with the infalling clumps to the standard mass accretion rate $\dot{M}_0 \sim 2\pi\nu\Sigma$ is

$$\frac{\dot{M}_\mathrm{p}}{\dot{M}_0} \ll \frac{1}{4\pi}\frac{R^2\Omega}{\nu} \sim \frac{1}{4\pi}\frac{u_\phi}{|u_R|} \gg 1. \tag{4}$$

Obviously, the restrictions on the mass input Ψ are rather weak. Formally, the change in Ω is larger for a much longer accretion time, $T_\mathrm{D} = R/|u_R| \sim R^2/\nu$ (here $u_R \sim \nu/R$ is explicitly assumed (Pringle, 1981)):

$$|\Delta\Omega| \sim \Omega_0 \frac{\dot{M}_\mathrm{p}}{\dot{M}_0}, \tag{5}$$

where Ω_0 is the characteristic angular velocity in the absence of mass loading.

For the radial velocity component we have

$$u_R \frac{\mathrm{d}u_R}{\mathrm{d}R} - \frac{u_\phi^2}{R} + \frac{1}{\rho}\frac{\mathrm{d}p}{\mathrm{d}R} + \frac{GM}{R^2} = -\frac{\Psi u_R}{\Sigma}. \tag{6}$$

Assuming that for a weak loading the radial component u_R is of the order of ν/R (Pringle, 1981) we arrive at

$$u_\phi^2 = \frac{GM}{R}[1 + \mathrm{O}(\mathcal{M}^{-2}) + \beta(R)], \tag{7}$$

where $\beta = \Psi u_R R^2/GM\Sigma$, $\mathcal{M} = u_\phi/c_\mathrm{s}$ is the local azimuthal Mach number and c_s is the local sound speed. Equations (2)–(6) differ from the standard equations of a thin accretion disc (Shakura and Sunyaev, 1973; Lyndel-Bell and Pringle, 1974) (see also reviews by Pringle (1981) and Papaloizou and Lin (1995)) in the sources due to mass loading in the right-hand side of the continuity equation (2) and in the radial velocity equation (6). The parameter β can be estimated as

$$\beta \sim \frac{\alpha}{\pi}\frac{T_\mathrm{R}}{T_\mathrm{D}}\frac{\dot{M}_\mathrm{p}}{\dot{M}_0} \ll 1, \tag{8}$$

with the assumption that $\dot{M}_{\rm p}/\dot{M}_0$ can have low or moderately high values; here α is the viscosity parameter (Shakura and Sunyaev, 1973), and thus its contribution to the right-hand side of equation (7) is negligible; in this sense the loading will be treated as weak. It is readily seen that $\beta \sim 2\pi\Psi/\Omega\Sigma$, and equation (8) is equivalent to the condition that, over one rotational period; $|\Delta\Omega| \ll \Omega$. This means that the infalling mass settles into generic Keplerian motion quickly and, as long as the mass input from the clumps is sufficiently small over one rotational period. Therefore equation (4) is fulfilled and can be treated as a weak loading.

Defining the accretion rate as $\dot{M} = -2\pi R\Sigma u_R$ (Pringle 1981), one can obtain the following solutions of equations (2) and (3) for a weakly loaded (i.e. $\beta \ll 1$) disc:

$$\dot{M} = \dot{M}_* - 2\pi \int_{R_*}^{R} \Psi R \, \mathrm{d}R, \tag{9}$$

$$v\Sigma = \frac{\dot{M}_*}{3\pi}\left[1 - \left(\frac{R_*}{R}\right)^{1/2}\right] - \frac{2}{3}\int_{R_*}^{R} \Psi R \, \mathrm{d}R, \tag{10}$$

where $\dot{M}_* = -2\pi(R\Sigma u_R)_*$ is the total mass accretion rate (i.e. the rate on the stellar surface); note that the mass rate provided by the accretion disc itself in the absence of mass loading is given by

$$\dot{M}_0 = \dot{M}_* - 2\pi \int_{R_*}^{\infty} \Psi R \, \mathrm{d}R. \tag{11}$$

The quantity $v\Sigma$ determines dissipation at a rate

$$D(R) = \frac{1}{2} v\Sigma (R\Omega')^2 = \frac{3GM\dot{M}_*}{8\pi R^3}\left[1 - \left(\frac{R_*}{R}\right)^{1/2}\right] - \frac{3GM}{4R^3}\int_{R_*}^{R} \Psi(R) R \, \mathrm{d}R, \tag{12}$$

and the corresponding luminosity integrated over the disc is

$$L_D^v = 4\pi \int_{R_*}^{\infty} D(R) R \, \mathrm{d}R = \frac{1}{2}\frac{GM\dot{M}_*}{R_*} - 3\pi GM \int_{R_*}^{\infty} \frac{\mathrm{d}R}{R^2} \int_{R_*}^{R} \Psi(R') R' \, \mathrm{d}R'. \tag{13}$$

2.3 Energy Equation

One of the most interesting and important consequences of the mass loading is connected with possible heating of the disc due to conversion of the kinetic energy of the falling gas into heat. The energy equation in the presence of mass loading (Cowie *et al.*, 1981; White and Long, 1991), integrated over z is written as

$$\Sigma\dot{\varepsilon} = \frac{3}{2}\frac{\mathcal{R}}{\mu} T\Psi\left(\frac{1}{2}(\gamma - 1)\frac{\rho\langle u^2\rangle}{p} - \gamma\right) + \frac{1}{2} v\Sigma (R\Omega')^2 - \mathcal{L}(T,\rho), \tag{14}$$

where ε is the specific (per unit mass) thermal energy. The first term on the right-hand side describes the energy input due to inelastic interaction of gas stripped from clumps and involved in Keplerian motion of the disc, $\langle u^2\rangle$ is the mean square relative velocity of the clumps and the disc (the averaging is over the ensemble of clumps), $\mathcal{R}$ is the gas constant, $\mathcal{L}$ is the radiative cooling rate (we shall assume that $\mathcal{L} = \sigma T^4$, where the σ is Stefan–

Bolzmann constant) and the second term is the dissipative energy rate (12). In the steady-state case, the disc temperature is determined from

$$\sigma T^4 = \frac{3}{2}\frac{\mathcal{R}}{\mu} T\Psi\left(\frac{1}{2}(\gamma-1)\frac{\rho\langle u^2\rangle}{p} - \gamma\right) + \frac{1}{2}\nu\Sigma(R\Omega')^2. \tag{15}$$

The mean square velocity is $\langle u^2\rangle = u_\phi^2 + u_c^2$, where u_c is the velocity dispersion of the clumps encountering the disc; for clumps orbiting around the central star or falling from external molecular cloud $u_c \approx u_\phi$, and so we shall assume that $\langle u^2\rangle \approx 2u_\phi^2$; the contribution from the radial disc velocity u_R is neglected. The corresponding contribution to disc luminosity from the first term on the right-hand side of equation (14) is

$$L_D^c = 6\pi\frac{\mathcal{R}}{\mu}\int_{R_*}^{\infty} T\Psi\left(\frac{1}{2}(\gamma-1)\frac{\rho\langle u^2\rangle}{p} - \gamma\right) R\,\mathrm{d}R \tag{16}$$

and, when compared with the viscous luminosity in the absence of mass loading, it is

$$\frac{L_D^c}{L_{D0}^v} \sim \frac{R^2\Psi}{\nu\Sigma} \sim \frac{\dot{M}_p}{\dot{M}_0}. \tag{17}$$

In dimensionless units, equation (15) is

$$\theta^4 + 6\delta\frac{\Lambda-1}{I}\psi\theta = 2(\gamma-1)\frac{\Lambda-1}{I}\frac{\psi}{x} + \frac{\Lambda}{x^3}\left(1 - \frac{1}{x^{1/2}}\right) - \frac{\Lambda-1}{I}\frac{1}{x^3}\int_1^x \psi x\,\mathrm{d}x, \tag{18}$$

where $x = R/R_*$, Ψ is assumed to be in the form $\Psi = \Psi_0\psi(x)$, $\theta = T/T_*$, $\delta = (c_*/c_M)^2$,

$$\begin{aligned} &T_* = \left(\frac{3GM\dot{M}_0}{8\pi\sigma R_*^3}\right)^{1/4}, \quad \Lambda = \frac{\dot{M}_*}{\dot{M}_0}, \quad \dot{M}_* = 2\pi\Psi_0 R_*^2 I + \dot{M}_0, \\ &I = \int_1^\infty \psi x\,\mathrm{d}x, \quad c_*^2 = \gamma\frac{\mathcal{R}}{\mu}T_*, \quad c_M^2 = \frac{GM}{R_*}. \end{aligned} \tag{19}$$

The problem contains two dimensionless parameters: δ and Λ. It is readily seen that $\delta \ll 1$; for $R_* = R_\odot$, $M = M_\odot$ and $\dot{M}_0 \approx 10^{-6} M_\odot\,\mathrm{year}^{-1}$ this ratio is $\delta \approx 10^{-3}$. For weak loading, $\dot{M}_* \gtrsim \dot{M}_0$, $\Lambda - 1$ is also small; however, even in this case, mass loading can significantly change the temperature distribution in the disc and its spectrum. In Figure 2 we show the temperature distribution $\theta(x)$ for the mass-loading function

$$\psi(R) = \left(\frac{R-R_*}{R_L}\right)\exp\left(-\frac{R-R_*}{R_L} + 1\right), \tag{20}$$

with the peak $\psi(R) = 1$ at $R = R_* + R_L$ (where R_L is the scale of the radial distribution of matter infall given by $R_L = LR_*$, $L = 30$) and for a set of Λ.

It is seen that the most important contribution from the additional mass input comes from regions with $x \gtrsim L$ where the temperature can increase by a factor of 2 even for a moderate

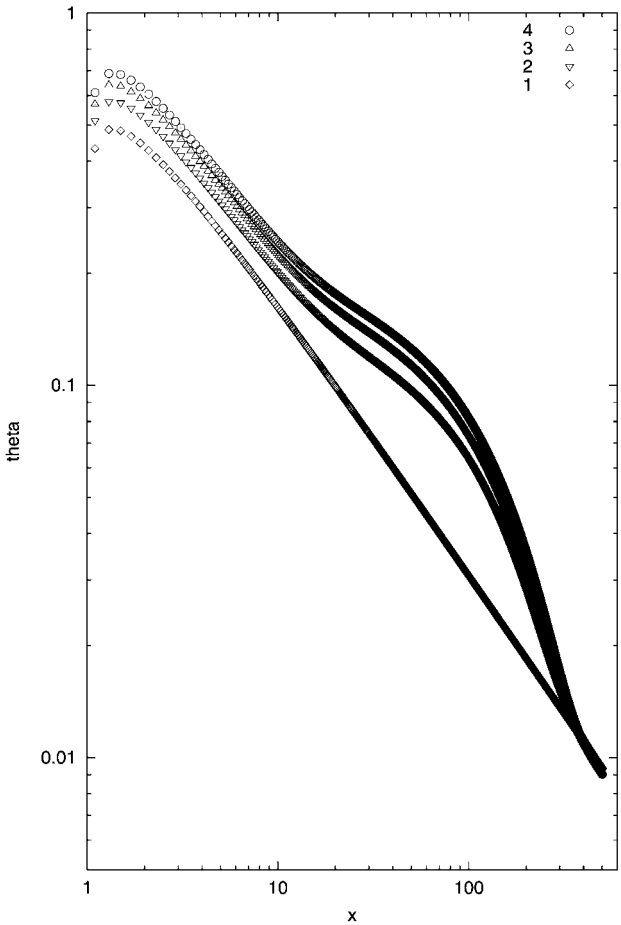

FIGURE 2 Temperature distribution $\theta(x)$ for the mass-loading function (20), with $\delta = 10^{-3}$, $\Lambda = 1$ (unloaded), 2, 3, 4 from the bottom to top and $L = 30$.

mass loading $\Lambda = 2$. At larger distances, $x \approx (10\text{–}20)L$, the temperature profiles for $\Lambda > 1$ approach the standard profile ($\Lambda = 1$) and then become lower because at such distances the heat input from kinetic energy of clumps ($u^2 \propto x^{-1}$, first term on the right-hand side of equation (18)) is smaller than the energy required to heat the infalling (presumably cold) gas (second term on the left-hand side of equation (18)). Similar changes are seen for a mass input more extended in radius, $L = 100$ (Figure 3). In this case, the surface mass input rate for equal Λ is about a third of that for $L = 30$, as $\Lambda - 1 \propto \Psi_0 L$; however, the increase in total luminosity of loaded discs from the area proportional to L^2 must be larger. For mass input in the form (20) and $\Lambda - 1 \approx 1$ at $x < L/3$, the second term on the right-hand side of equation (18) dominates and the first and third terms contribute only around 0.01–1%; at $x \gtrsim L/3$, the situation changes and the main contribution (up to 97%) is from the first term in equation (18). At $x > 10L$, the dominant contribution is again from the second term; the third term at $x > L/3$ always remains about 30–50% of the second term. For $\Lambda - 1 \approx 0.1$ the second term dominates up to $x \approx 2L/3$ and then, at $x > 8L$, the last term always remains as small as 5–10% of the second term.

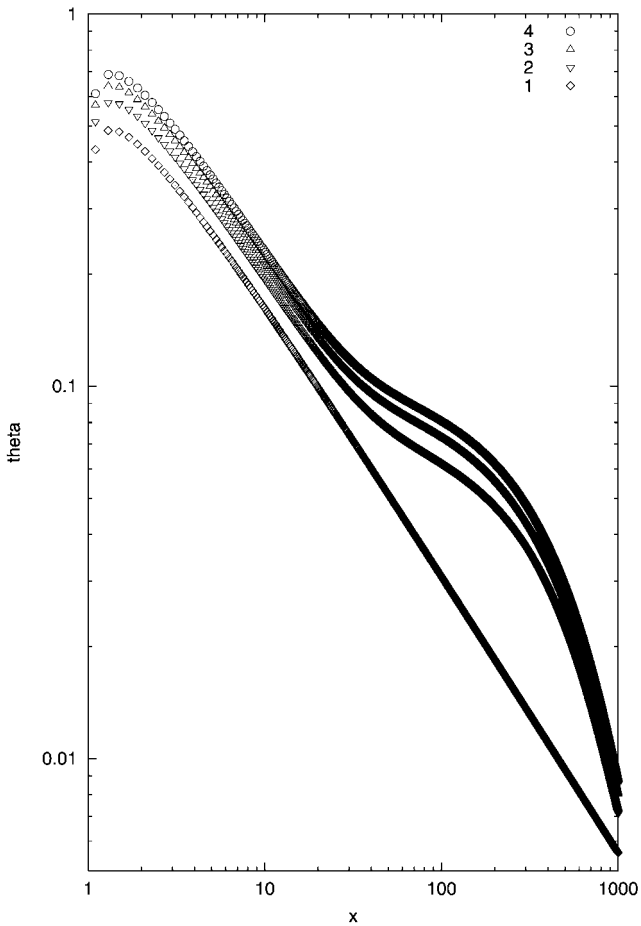

FIGURE 3 Same as Figure 2 but for $L = 100$.

In order to illustrate how the mass loading can change the spectra of accretion discs, we show here the spectral energy distribution (SED) for optically thick discs seen face on:

$$\Sigma_\nu = 2\pi \int_{R_*}^{R_{\rm out}} B_\nu[T(R)] R \, {\rm d}R, \tag{21}$$

with $T(R) = T_* \theta(x)$, $B_\nu[T(R)]$ being the Planck function and $R_{\rm out}$ being the outer radius of the disc; in the models shown in Figures 2–5, $R_{\rm out} = 500$, and the contribution from regions with $R > 500$ is small. Defining the dimensionless frequency y as

$$y = \frac{h\nu}{k_{\rm B} T_*}, \tag{22}$$

one can reduce equation (21) to the form

$$\Sigma_\nu = \Sigma_0 S(y), \tag{23}$$

where

$$\Sigma_0 = \frac{16\pi^2 k_B^3 T_*^3 R_*^2}{h^2 c^2}. \tag{24}$$

Figure 4 shows the spectra from discs with the temperature distribution shown in Figure 2. It is seen that, even for a relatively small loading, $\Lambda = 2$, the spectrum changes substantially: at the maximum it increases by a factor of 5; the maximum itself is sharper, showing an excess of energy in this range (for $R = R_\odot$, $M = M_\odot$ and $\dot{M}_0 = 10^{-6} M_\odot$ year^{-1} the frequency at the maximum is $\nu \approx (1\text{–}1.5) \times 10^{13}$ Hz or $\lambda \approx 10\text{–}20\,\mu$m). For a more extended disc ($L = 100$) the changes in their spectra are more pronounced as shown in Figure 5: at $\Lambda = 2$ at the maximum it increases by an order of magnitude in comparison with mass-unloaded discs, the maximum itself shifts to a lower frequency, and the energy excess in this frequency range is more obvious. These two examples show that additional heat input due to mass loading can be responsible for (or may contribute to) the far-infrared (FIR) excess observed from circumstellar discs around young stars (see for a review Natta *et al.* (1997)). In order to illustrate such a possibility we compare in Figure 6 the spectrum expected from an optically thick

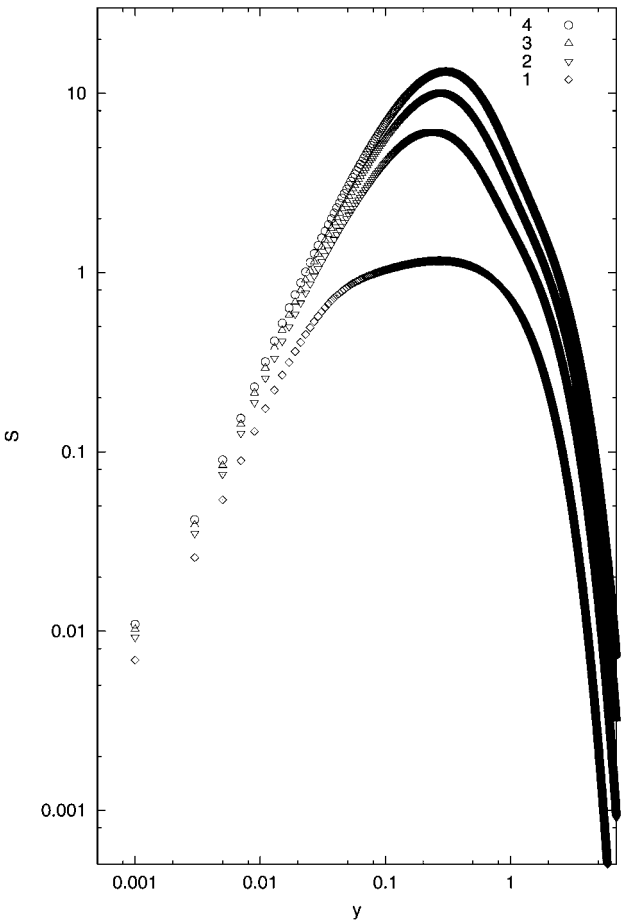

FIGURE 4 Energy spectrum for the $\theta(x)$ shown in Figure 2.

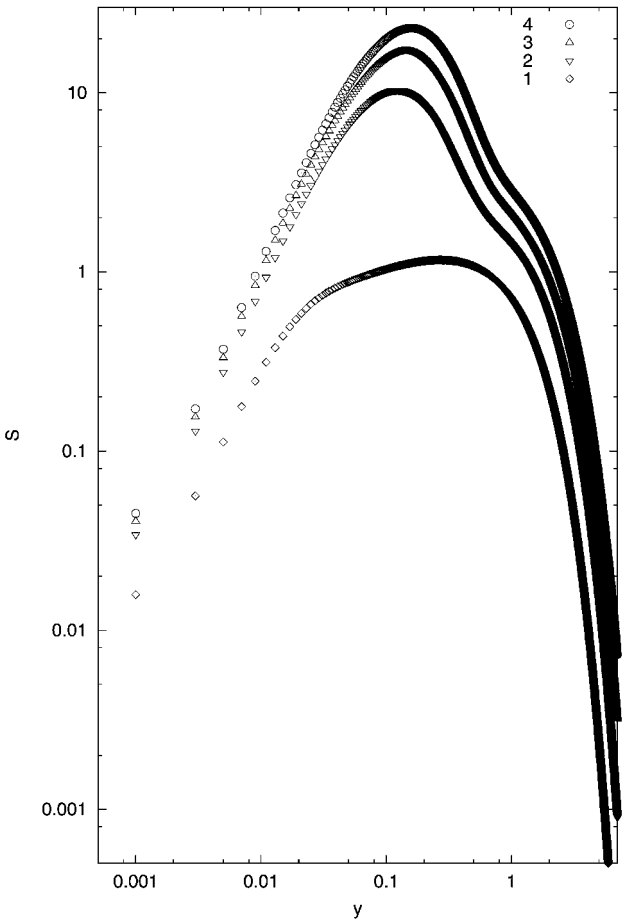

FIGURE 5 Same as in Figure 4 but for $L = 100$.

mass-loaded disc seen face on with that observed in the Chameleon cloud (Natta *et al.* 1997). For the modelled spectrum we assumed the distribution of infalling material with a radius of $L = 9.2\,\mathrm{AU}$ (integration was over $R = 3L$), an accretion mass rate $\dot{M}_0 = 2.2 \times 10^{-7} M_\odot\,\mathrm{year}^{-1}$ and mass loading only $\Lambda - 1 = 0.08$; the central star has $M = 1M_\odot$ and $R_* = R_\odot$. Full squares show the FIR excess observed from CS Chameleon, which cannot be attributed to a standard reprocessing accretion disc; open diamonds presumably show the photospheric emission. (The lack, or negligibly low level, of emission in the optical and near-infrared range from the accretion disc is considered to be an indication of a hole in the inner disc (about 0.3 AU in size).)

For a rough estimate of the effects of mass loading on SEDs from accretion discs, one can use the following approximate expression for temperature in the region where heating, due to dissipation of kinetic energy of falling clumps (first term on the right-hand side of equation (18)), reaches a maximum (at $x_\mathrm{m} \sim L^{1/2}$ with $(s/x)_\mathrm{m} \sim e/L$);

$$\theta_\mathrm{m} \sim \left(2(\gamma - 1)\frac{\Lambda - 1}{I}\frac{e}{L}\right)^{1/4}, \tag{25}$$

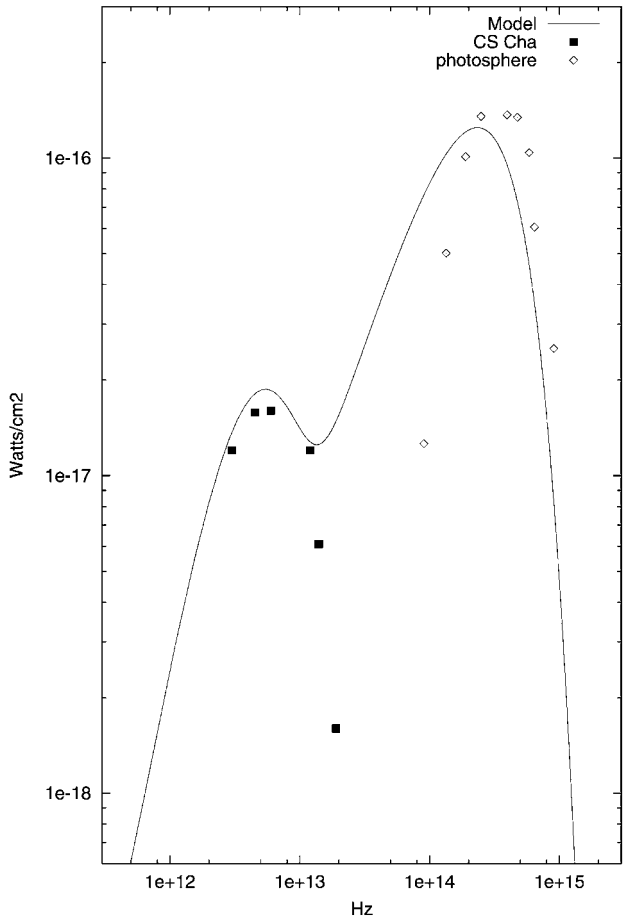

FIGURE 6 SED in CS Cha: ◇, from ground-based observations (presumably representing the spectrum of the stellar photosphere); ■, from ISO and IRAS (Natta *et al.*, 1997); —, the spectrum of a mass-loaded disc with $\Lambda = 1.08$, $L = 9.2\,\mathrm{AU}$ and $\dot{M}_0 = 2.2 \times 10^{-7} M_\odot\,\mathrm{year}^{-1}$.

which is of the correct order of magnitude to describe the asymptotics at distances x where accretion heating (last two terms in equation (18)) and cooling due to mixing of cold infalling gas (second term on the left-hand side of equation (18)) are unimportant; this region corresponds to the plateaux in the $\theta(x)$ profiles in Figures 2 and 3. In dimensional units, $T_\mathrm{m} \sim 0.8(\Lambda - 1)^{1/4} L^{-1/2} T_*$. For the above model this gives $T_\mathrm{m} \approx 100\,\mathrm{K}$, and the corresponding frequency $\nu_\mathrm{m} \approx 6 \times 10^{12}\,\mathrm{Hz}$.

2.4 Effects of Angular Momentum Input

When the infalling gas has a non-zero angular momentum equation, so that $v_{\mathrm{c},\phi} \neq 0$, equation (3) is written in the form (Safronov and Vityazev, 1983; Papaloizou and Lin, 1995)

$$\frac{\mathrm{d}}{\mathrm{d}R}(\Sigma R^3 \Omega u_R) = \frac{\mathrm{d}}{\mathrm{d}R}\left(\nu \Sigma R^3 \frac{\mathrm{d}}{\mathrm{d}R}\Omega\right) + \Psi(R) R^2 v_{\mathrm{c},\phi}(R), \tag{26}$$

and the contribution to the energy equation is determined by

$$\frac{2\pi}{\dot{M}_0 R^2 \Omega} \int_{R_*}^{R} \Psi(R) R^2 v_{c,\phi}(R)\, dR. \tag{27}$$

In the extreme case when the angular velocity of the infalling gas approaches the Keplerian value $v_{c,\phi}(R) = (GM/R)^{1/2}$ the energy equation is

$$\theta^4 + 6\delta \frac{\Lambda - 1}{I} \psi\theta = 2(\gamma - 1)\frac{\Lambda - 1}{I}\frac{\psi}{x} + \frac{\Lambda}{x^3}\left(1 - \frac{1}{x^{1/2}}\right) - \frac{\Lambda - 1}{I}\frac{1}{x^3}\int_1^x \psi x\, dx + \frac{\Lambda - 1}{I}\frac{1}{x^{7/2}}\int_1^x \psi x^{3/2}\, dx. \tag{28}$$

It is readily seen that for a mass input rate in the form (20) the contribution from the last term is of the same order of magnitude as (about two thirds of) the third term and thus never exceeds 30% for $\Lambda \approx 1$ and 3–6% for $\Lambda - 1 \ll 1$.

3 CONCLUSIONS

Dissipation of the kinetic energy of a clumpy gas falling on to accretion discs from the debris of a parent protostellar molecular cloud significantly alters the radial temperature distribution. It can be important in outer parts of a reprocessing disc, where the temperature decreases sufficiently, $T \sim R^{-3}$, while the heat input rate associated with mass loading is approximately proportional to the square of the azimuthal velocity, $\dot{E} \propto R^{-1}$. Thus, mass loading can naturally produce an excess of emission in the long-wavelength range of SEDs of the accretion discs and, with an appropriate radial distribution of mass loading, reproduce the observed FIR excess. For a one-peak radial distribution of the infall rate localized at $R \approx L$, the corresponding temperature in the hot ring for $R_* = 1R_\odot$ and $M_* = M_\odot$ is

$$T_m \sim 800\left(\frac{\dot{M}_p}{\dot{M}_0}\right)^{1/4}\left(\frac{L}{1\,\mathrm{AU}}\right)^{-1/2}\left(\frac{\dot{M}_0}{10^{-6}M_\odot\,\mathrm{year}^{-1}}\right)^{1/4}\mathrm{K}, \tag{29}$$

and the wavelength

$$\lambda_m \sim 6\left(\frac{L}{1\,\mathrm{AU}}\right)^{1/2}\left(\frac{\dot{M}_p}{\dot{M}_0}\right)^{-1/4}\left(\frac{\dot{M}_0}{10^{-6}M_\odot\,\mathrm{year}^{-1}}\right)^{-1/4}\mu\mathrm{m}. \tag{30}$$

It is readily seen that the extra luminosity produced by the infalling gas is proportional to the mass loading rate, $L(\dot{M}_p) \sim \sigma T_m^4 L^2 \propto \dot{M}_p$, and for weak mass loading, $\dot{M}_p \ll \dot{M}_0$, is small compared with the total luminosity of an unloaded disc. However, it can result in an observable effect if the loading mass is deposited at large radii, so that the wavelength in the peak of emission (30) falls into the FIR range where the reprocessing disc does not contribute significantly. This case is shown in Figure 6 where, for the mass loading $\dot{M}_p \approx 0.1\dot{M}_0$, the FIR luminosity of the infalling gas is approximately a tenth of the optical luminosity of the reprocessing disc.

The results presented in this paper have only an illustrative meaning and can be directly applied to explain the spectral features observed in protoplanetary discs only when clear evi-

dence of mass loading is found. Nonetheless, they definitely show that mass loading can have an important influence on the temperature distribution in accretion discs and their spectra.

Note added in proofs

After acceptance of this paper I have been informed about the papers by Falcke, H. & Melia, F. (1997) *Astrophys. J.*, **479**, 740, and Coker, R. F., Melia, F. & Falcke, H. (1999) *Astrophys. J.*, **523**, 642 which deal with accretion discs around massive black holes loaded by wind infall in the framework of hydrodynamical equations similar to that used in this paper, with application to Sgr A*. Their emission spectrum has an excess in the long-wavelength limit due to additional energy input connected with the mass-loading similar to that obtained in our paper.

Acknowledgements

I thank S. A. Lamzin, A. V. Lapinov, A. M. Sobolev and I. I. Zinchenko for valuable discussions. This work was supported by RFBR (project 99-02-16938) and INTAS (project 1667). This research has made use of the Astrophysics Data System Abstract Service, National Aeronautics and Space Administration.

References

Barnes, S., Tobin, W. and Pollard, K. R. (2000) *Publ. Astron. Soc. Aust.*, **17**, 241.
Cowie, L. L., McKee, C. F. and Ostriker, J. P. (1981) *Astrophys. J.*, **247**, 908.
Falgarone, E., Phillips, T. G. and Walker, C. K. (1991) *Astrophys. J.*, **378**, 186.
Grinin, V., Natta, A. and Tambovtseva, L. (1996) *Astron. Astrophys.*, **313**, 857.
Hartquist, T. W., Dyson, J. E., Pettini, M. and Smith, L. J. (1986) *Mon. Not. R. Astron. Soc.*, **221**, 715.
Klein, R. I., McKee, C. F. and Colella, P. (1994) *Astrophys. J.*, **420**, 213.
Lecavelier des Etangs, A., Hobbs, L. M., Vidal-Madjar, A., Beust, H., Feldman, P. D., Ferlet, R., Lagrange, A.-M., Moos, W. and McGrath, M. (2000) *Astron. Astrophys.*, **356**, 691.
Lynden-Bell, D. and Pringle, J. E. (1974) *Mon. Not. R. Astron. Soc.*, **168**, 603.
Natta, A., Meyer, M. R. and Beckwith, S. V. W. (1997) In: Zun, J. and Liseau, R. (eds), *Star Formation with the Infrared Space Observatory*, ASP Conference Series, Vol. 132, p. 265.
Papaloizou, J. C. B. and Lin, D. N. C. (1995) *A. Rev. Astron. Astrophys.*, **33**, 505.
Pringle, J. E. (1981) *A. Rev. Astron. Astrophys.*, **19**, 137.
Roberge, A., Feldman, P. D., Lagrange, A. M., Vidal-Madjar, A., Ferlet, R., Jolly, A., Lemaire, J. L. and Rostas, F. (2000) *Astrophys. J.*, **538**, 904.
Safronov, V. S. and Vityazev, A. V. (1983) In: R. A. Sunyaev (ed.), *Astrophysics and Cosmic Physics*, p. 5.
Shakura, N. I. and Sunyaev, R. A. (1973) *Astron. Astrophys.*, **24**, 337.
White, R. L. and Long, K. S. (1991) *Astrophys. J.*, **373**, 543.